Probability of spacecraft's 1:1 ground-track resonance capture around an asteroid with the adiabatic invariant theory

Wail Boumchita[1, a] **and Jinglang Feng**[1, b]

[1] *Department of Mechanical and Aerospace Engineering (Aerospace Center of Excellence), University of Strathclyde, 75 Montrose Street, Glasgow G1 1XJ, United Kingdom.*

[a] *wail.boumchita@strath.ac.uk*
[b] *jinglang.feng@strath.ac.uk*

Abstract

Vesta is the second largest celestial object of the main asteroid belt and it was visited and investigated by the DAWN mission in 2011. The spacecraft used solar-electric propulsion that generates continuous low-thrust. As the spacecraft slowly descends from high altitude mission orbit (HAMO) to low altitude mission orbit (LAMO), it crosses the 1:1 ground-track resonance, putting the spacecraft at risk of being permanently trapped into it. The objective of this paper is to apply the adiabatic invariant theory to estimate the Dawn's probability of capture into 1:1 ground-track resonance with Vesta. Firstly, we define the averaged Hamiltonian considering the irregular gravitational field up to the second order and degree and the thrust constant in magnitude and opposite to the velocity direction of the spacecraft. Then, we expand the model around the resonance which results the Hamiltonian to be reduced into the first fundamental resonance model, a time-dependent one-degree of freedom Hamiltonian. The phase-space topology changes due to the time-dependency causing the area enclosed by the separatrices to grow. This is the cause of trapping into resonance and, based on the dynamical system's energy change, an intuitive definition of probability of captured is presented. Finally, we adapt the probability definition to be used with the first fundamental model, estimate the Dawn's probability of capture into 1:1 ground-track resonance around Vesta and validate it with Monte Carlo simulations.

Keywords: Adiabatic invariant theory, Resonance capture, Astrodynamics, Vesta, Gravitational perturbations, Low-thrust propulsion

1 Introduction

In 2011, the Dawn spacecraft successfully approached the asteroid Vesta [1]. The DAWN mission was one of the first missions to use low-thrust propulsion during both the cruise phase and the approach phase to an asteroid. It demonstrates the possibility of relying on low-thrust propulsion for the majority of the mission duration. As the spacecraft slowly approaches the asteroid, there is a possibility that it is captured by the 1:1 ground-track resonance and being permanently trapped into it. An example of 1:1 ground-track resonance is the geostationary orbit, in which the period of revolution of the spacecraft is equal to the period of rotation of the Earth around its axis. However, the motion around Vesta is more complex, being smaller in size and having a more irregular gravitational field and the spacecraft at each revolution encounters the same gravitational configuration, the effect of which accumulates over the revolutions and change noticeably the orbit eccentricity and inclination. Small variations in the initial state of the spacecraft can make a difference in whether the spacecraft manages to cross the resonance and reach lower altitudes from if the spacecraft remains trapped in the resonance despite the continuous thrusting. Since the application of the low-thrust propulsion is the future tendency, the study of the probability of capture into resonance of a spacecraft around a celestial body needs to be investigated. Delsate [2] defined the autonomous Hamiltonian which describes the 1:1 resonance around Vesta for both circular polar orbits and circular equatorial orbits.

The adiabatic invariant theory is a useful semi-analytical approach to estimate the probability of capture into resonance of a dynamical system if the system's Hamiltonian is dependent on slowly changing parameters over time, for example a pendulum which length slowly changes with time. The theory is based on the fact that the trajectory of the non autonomous system is close to the trajectory of the autonomous system, but slowly drifting from it. The only information required a priori is the initial state of the system and an assumption on the rate of change of the parameter. Usually, to estimate the probability of capture of a dynamical system the first fundamental resonance model has been adopted [3] [4]. Henrard [5] [6], in the context of celestial mechanics, Neishtadt [7], in the contexts of physical systems in planetary science and plasma physics, and Kruskal, privately communicated to Dobbrot and Greene [8] for the motion of charged particles in stellarators for fusion power generation, independently defined the expression of the probability of capture into resonance based on Liouville's theorem, which states that time evolution in phase space is an incompressible flow even if the Hamiltonian is time dependent. A straightforward expression of the probability of capture can be used if the Hamiltonian system is reduced to the first fundamental resonance model. Breiter [9] reviewed the process of reducing the system's Hamiltonian to the different fundamental resonance models and Artemyev [10] did a review of the adiabatic invariant theory presenting application of it in different fields. Boccaletti and Pucacco [11] dedicated a chapter of their book to this methodology, applying it to the case of one-degree of freedom systems and many degree of freedom systems.

With this work, we extend the above research and we advance the knowledge about this phenomenon by developing a new Hamiltonian model without restrictions on the inclination and eccentricity of the orbit and process it in order to be used for the first time in the context of the adiabatic invariant theory. This paper is structured as follows. In Section 2, we define the equations of motion describing the dynamics of the spacecraft's motion around Vesta. Section 3 outlines the estimation process of the adiabatic invariant theory. Section 4 applies the theory developed in the previous section to estimate the Dawn's probability of capture into 1:1 resonance around Vesta. Finally, Section 5 concludes this study.

2 Numerical model

In this section we define the equations of motion of a spacecraft moving around a uniformly rotating asteroid. The model considered is the two-body problem with perturbations from the irregular gravitational field of the asteroid and the low-thrust to which the spacecraft is subject to. The gravitational field is represented by the spherical harmonics model and is truncated to the second order and degree, the low-thrust is constant in magnitude and it always directs to the opposite direction of the spacecraft's velocity, which maximizes the instantaneous variation of orbital energy. Following Kaula [12] , the potential of the gravitational field of an asteroid V in spherical coordinates can be expressed as the sum of the keplerian component and a spherical harmonic expansion up to the degree n and order m

$$V = \frac{\mu}{r} + \sum_{n=2}^{\infty}\sum_{m=0}^{n} \frac{\mu}{r}\left(\frac{R_e}{r}\right)^n P_{nm}(\sin\phi) \\ (C_{nm}\cos m\delta + S_{nm}\sin m\delta) \quad (1)$$

where μ is Vesta's gravitational constant, R_e is the reference radius of the asteroid, $P_{n,m}(\sin\phi)$ are the associated legendre polynomials, r is the radial distance, ϕ is the latitude, δ is the longitude, C_{nm} and S_{nm} are the spherical harmonics coefficients and n and m are integers.

By transforming the potential in cartesian coordinate and taking the gradient of the potential and adding the low thrust component to the acceleration, we can define the equations of motion which describe the absolute spacecraft's motion in the asteroid centered inertial frame as Eq.2 where V represents the potential expanded in spherical harmonics as a function of the cartesian coordinates (x, y, z), T is the thrust, m is the spacecraft's mass and $\hat{\boldsymbol{v}}$ is the spacecraft's velocity unit vector. To that, we add the differential equation describing the rate of change of the spacecraft's mass over time as Eq.3 where I_{sp} and g_0 represent the specific impulse if the engine and standard free-fall acceleration respectively.

$$\ddot{\boldsymbol{x}} = \boldsymbol{\nabla} V - \frac{T}{m(t)}\hat{\boldsymbol{v}} \quad (2)$$

$$\dot{m} = -\frac{T}{I_{sp} g_0} \quad (3)$$

We consider the initial conditions in Table 1.

Table 1: DAWN spacecraft initial conditions at its arrival at Vesta.

Mass (m_0)	1000 kg
Thrust (T)	20 mN
Specific Impulse (I_{sp})	3000 s
SMA (a_0)	1000 km
eccentricity (e_0)	0
Inclination (i_0)	90°
Longitude of the ascending node (Ω_0)	0°
Argument of periapsis (ω_0)	0°

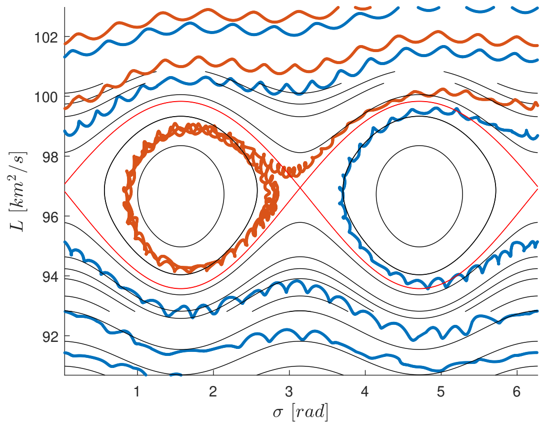

Figure 1: Spacecraft trajectory in the (σ, L) plane. The red line represents the capture case starting at $\theta_0 = 30°$ and the blue line represents the escape case with $\theta_0 = 50°$.

We focus on the 1:1 resonance and we numerically estimate the probability of capture considering 1000 different values of initial true anomalies (θ_0). The 1:1 resonance capture bounds the motion of the spacecraft inside the resonance region, not allowing it to reach lower altitudes. The outcome of the simulations indicates that if the descent starts at 1000 km and the low-thrust magnitude is 20 mN, the probability of capture of the spacecraft into 1:1 resonance around Vesta is estimated to be $\sim 8.6\%$. The value is coherent with what was previously found by Delsate [2] and Tricarico [13], thus validating our model.

The capture into resonance is a phenomenon that depends on the initial phase angle of the descent. For the analysis, we consider two different values of initial true anomalies to represent the case in which the spacecraft is capture into resonance and the case in which it escapes:

$$\begin{cases} \theta_0 = 30°, & \text{for the capture case} \\ \theta_0 = 50°, & \text{for the escape case} \end{cases} \tag{4}$$

It is possible to represent the results of these two cases in the phase space, in which the x-axis represents the resonance angle $\sigma = \psi - \vartheta$ defined as the difference between the mean longitude and the angle of rotation of the planet, while the y-axis represents the angular momentum L.

Notice the different behaviour of the phase space trajectory between the two cases: for the first case in Figure 1, with $\theta_0 = 30°$, the trajectory remains inside the region between the upper and lower separatrices (lines highlighted with the red color), which corresponds to the 1:1 resonance; for the second case, with $\theta_0 = 50°$, the trajectory crosses the upper separatrix and immediately crosses the lower one, thus escaping from the resonance. The results from the numerical simulations are characterized with large oscillations, for this reason we use the MATLAB function `movmean` with a window length of 200 to smooth the results and have a better visualization of the phase space trajectory.

3 Adiabatic invariant theory

Formally [14], a variable $I(p, q, \lambda)$ is recognized as an adiabatic invariant if, for every $\epsilon > 0$ there exist a $\delta_\epsilon > 0$ so that, for every $\delta < \delta_\epsilon$ and $t < 1/\delta$

$$|I(p(t), q(t), \delta t) - I(p_0, q_0, 0)| < \epsilon \tag{5}$$

which means that for a time variation of almost $1/\epsilon$, the adiabatic invariant changes in the order of ϵ.

The adiabatic invariant theory (AIT) was initially introduced in the field of quantum mechanics, to give a more solid bases to the quantisation rules [11]. Later on, the theory was found useful also in the field of celestial mechanics due to the possibility for many system's Hamiltonian to be transformed to the first fundamental resonance model, a pendulum-like Hamiltonian [6] [15] defined as

$$\mathcal{H} = \frac{1}{2}p^2 - b\cos q \tag{6}$$

The Hamiltonian generally has one degree of freedom and depends on slowly varying parameters. By providing realistic assumption on how the parameters change over time, the AIT can provide precise information regarding the dynamical system's long term evolution. Taking as reference Figure 1, the separatrices are the red curves that separates the two circulation zones from the libration one. During the evolution of the dynamical system the separatrices move, expanding the libration region. This area variation is directly correlated with the probability of capture. In particular, the first fundamental resonance model was studied in depth, defining analytically the area variation of the libration region with respect to the slowly changing parameter and the probability of capture into resonance. For this reason, we initially reduce the Hamiltonian in this model from the complete Hamiltonian model.

3.1 Hamiltonian model

3.1.1 Natural Hamiltonian

The Hamiltonian of a spacecraft descending towards an asteroid with irregular gravitational field using low-thrust includes a gravitational component and a low-thrust one. The gravitational field previously defined in Eq. 1 can be expressed as a function of the orbital parameters such as

$$V = \frac{\mu}{r} + \sum_{n=2}^{\infty}\sum_{m=0}^{n}\sum_{p=0}^{n}\sum_{q=-\infty}^{\infty} \frac{\mu R_e^n}{a^{n+1}} F_{nmp}(i) G_{npq}(e) S_{nmpq}(\omega, M, \Omega, \theta) \quad (7)$$

where r is the distance between the spacecraft and the asteroid, $F_{nmp}(i)$ is a function of the inclination, $G_{npq}(e)$ is a function of the eccentricity, ω is the argument of periapsis, M is the mean anomaly, Ω is the longitude of the ascending node, θ is the sidereal time, n, m, p and q are all integers and

$$S_{nmpq} = \begin{cases} C\cos\Psi + S\sin\Psi & \text{if } n-m \text{ is even} \\ -S\cos\Psi + C\sin\Psi & \text{if } n-m \text{ is odd} \end{cases} \quad (8)$$

where we dropped the indices for C, S and Ψ and Ψ_{nmpq} is the Kaula's phase angle

$$\Psi_{nmpq} = (n-2p)\omega + (n-2p+q)M + m(\Omega - \theta) \quad (9)$$

Resonances arise when the time derivative of Kaula's phase angle $\dot{\Psi}_{nmpq}$ is approximately null.

By defining $L = \sqrt{\mu a}$ as the moment conjugated to the mean longitude ψ, it is possible to define the Hamiltonian that describes the motion of the spacecraft around an asteroid with an irregular gravitational field as

$$\mathcal{H} = -\frac{\mu^2}{2L^2} + \sum_{n=2}^{\infty}\sum_{m=0}^{n}\sum_{p=0}^{n}\sum_{q=-\infty}^{\infty} \mu\frac{R_e^n}{a^{n+1}} F_{nmp}(i) G_{npq}(e) S_{nmpq}(\omega, M, \Omega, \theta) + \dot{\theta}\Lambda \quad (10)$$

where $\dot{\theta}$ is the rotation rate of the asteroid and Λ is the conjugated momentum of θ.

The harmonic contributions that are included in the potential V are those associated with the resonance under consideration. In general, for a k_1:k_2 resonance the following constraints must be satisfied

- n, m, p and q must be integer numbers;
- in case the orbit is circular $q = 0$;
- p has to meet the following relation derived from Kaula's phase angle

$$p = \frac{1}{2}\left(n - \frac{k_2}{k_1}m\right)$$

For an gravity field modelled up to the second degree and order, the term that contribute to the resonance are the ones associated with C_{20} and C_{22}. In particular, the resonance is due to the tesseral harmonic C_{22} and for this reason, initially, we do not consider the zonal harmonic C_{20}. In Section 4, we analyze how the results changes with and without the gravitational term associated to C_{20}. The Hamiltonian associated to the 1:1 resonance and containing the gravitational term up to the second order is given as

$$\mathcal{H}_{nat} = -\frac{\mu^2}{2L^2} + R_e^2 \frac{\mu}{a^3(t)} F_{220} G_{200} C_{22}\cos[2(\psi - \theta)] + \dot{\theta}\Lambda \quad (11)$$

and the inclination and eccentricity functions are defined as

$$\begin{cases} F_{220} = \frac{3}{4}\left(1 + \cos i\right)^2 \\ G_{200} = \left(1 - \frac{5}{2}e^2 + \frac{13}{16}e^4\right) \end{cases} \quad (12)$$

Following [2][16], we define the resonance angle σ related to the 1:1 resonance

$$\sigma = \psi - \theta \quad (13)$$

We consider a symplectic transformation which leads to the new set of canonical variables

$$\sigma \quad , \quad L' = L \quad , \quad \theta' = \theta \quad , \quad \Lambda' = \Lambda + L \quad (14)$$

and by selecting only the resonant contributions, the new Hamiltonian is defined as

$$\mathcal{H}_{nat} = -\frac{\mu^2}{2L^2} - R_e^2 \frac{\mu}{a^3(t)} F_{220} G_{200} C_{22} \cos 2\sigma - \dot{\theta} L \quad (15)$$

3.1.2 Perturbed Hamiltonian

The work per unit mass done by the low-thrust is expressed as

$$\mathcal{H}_{LT} = -\tau_{LT}\psi = -|\boldsymbol{r} \times \boldsymbol{a}_{LT}|\psi = = -\frac{T}{m} r\psi \sin(-\pi/2 - \gamma) \sim \frac{T}{m} a\psi$$

where $\boldsymbol{a}_{LT}$ is the acceleration vector due to the low-thrust and always directed opposite to the velocity vector, T is the magnitude of the thrust, m is the instantaneous spacecraft's mass, a is the semi-major axis (SMA), and γ the flight path angle. Numerically, for the case considered in this paper in Section 4, the flight path angle does not exceed $5°$ as in Figure 2.

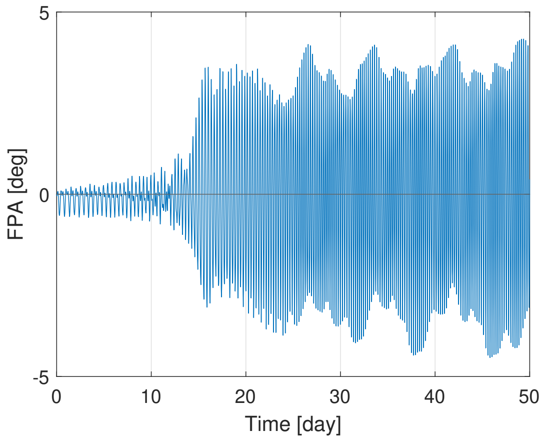

Figure 2: Flight path angle (FPA) profile during Dawn's descent.

Using the definition of σ

$$\mathcal{H}_{LT} = \frac{T}{m} a(\sigma + \theta) \sim \frac{T}{m} a\sigma \tag{16}$$

in which the term related to the fast angle θ was neglected to make the Hamiltonian dependent only on σ. So the complete Hamiltonian is given as

$$\mathcal{H}_{1:1} = \mathcal{H}_{nat} + \mathcal{H}_{LT} = \tag{17}$$

$$= -\frac{\mu^2}{2L^2} - R_e^2 \frac{\mu}{a^3(t)} F_{220} G_{200} C_{22} \cos 2\sigma - \dot{\theta} L + \frac{T}{m}\frac{L^2}{\mu}\sigma \tag{18}$$

3.1.3 Slowly changing parameter definition

Starting from the Hamiltonian defined in Eq.15, we focus on the term related on the gravitational term associated to the second order and degree $\mathcal{H}_{22}$

$$\mathcal{H}_{22} = -R_e^2 \frac{\mu^4}{a^3(t)} F_{220} G_{200} C_{22} \cos 2\sigma \tag{19}$$

We choose to consider the SMA as slowly varying, so

$$a(t) = a_0 - \dot{a}t = a_0(1 - \frac{\dot{a}}{a_0}t) = \tag{20}$$

$$= a_0(1 - \epsilon t) = a_0(1 - \lambda) \tag{21}$$

where we define the parameters as $\epsilon = \frac{\dot{a}}{a_0}$ and $\lambda = \epsilon t$ and a_0 is the initial value of the SMA. Therefore, we define $\mathcal{H}_{22}$ as

$$\mathcal{H}_{22} = -R_e^2 \frac{\mu^4}{a_0^3(1-\lambda)^3} F_{220} G_{200} C_{22} \cos 2\sigma \tag{22}$$

Numerically, the SMA evolves as in Figure 3.

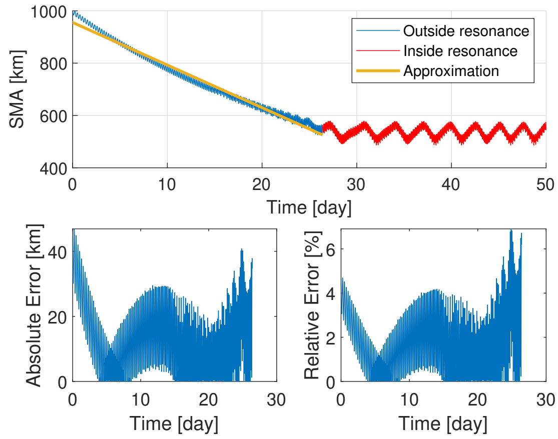

Figure 3: SMA evolution (blue line) and its approximation (yellow line). Below are reported the absolute and relative error between the real and approximated SMA evolutions.

The yellow line in Figure 3 can be considered a good approximation on the rate of change of the SMA. In fact, the maximum relative error between the real and approximated SMA evolution is $\sim 6\%$. The slope of the linear approximation, corresponding to the rate of change of the SMA, is numerically estimated to be

$$|\dot{a}| \sim 10^{-4} \text{km/s} \tag{23}$$

so

$$\epsilon = \frac{|\dot{a}|}{a_0} \sim 10^{-7} \text{1/s} \tag{24}$$

which satisfies the condition that $\epsilon \ll 1$. So, defining $q = 2\sigma$ and $L_0 = \sqrt{\mu a_0}$, the model that we will consider in Section 4 to estimate the probability of capture is

$$\mathcal{H}_{1:1} = -\frac{\mu^2}{2L^2} - R_e^2 \frac{\mu^4}{L_0^6(1-\lambda)^3} F_{220} G_{200} C_{22} \cos q - \dot{\vartheta} L + \frac{1}{2}\frac{T}{m}\frac{L^2}{\mu} q \tag{25}$$

3.2 Hamiltonian model expansion

The second part of the estimation process involves the expansion of the Hamiltonian around the resonance and its reduction to the first fundamental resonance problem.

We search for the equilibria location L_{eq} as solution of

$$\frac{\partial \mathcal{H}}{\partial L} = 0 \tag{26}$$

around which the expansion is performed. The full Hamiltonian model in Eq.15 related to the 1:1 resonance is divided in three parts $\mathcal{H}_0$, $\mathcal{H}_{22}$ and $\mathcal{H}_{LT}$ defined as

$$\mathcal{H}_{1:1} = \mathcal{H}_0 + \mathcal{H}_{22} + \mathcal{H}_{LT} \tag{27}$$

The expansion is implemented at two different orders: we expand $\mathcal{H}_0$ up to the second order with respect to L_{eq}, while $\mathcal{H}_{LT}$ is expanded up to the zero order with respect to L_{eq}. This procedure leads to the following expressions

$$\mathcal{H}_0^* = \frac{1}{2}\mathcal{H}_0^{''}|_{L_{eq}}(L - L_{eq})^2 \tag{28}$$

$$\mathcal{H}_{LT}^* = \mathcal{H}_{LT}|_{L_{eq}} \tag{29}$$

where $'$ indicates the derivative with respect to L. Near the resonance $\mathcal{H}_0^{'} = 0$ and the constant term in $\mathcal{H}_0^*$ does not contribute to the dynamics. The reason for this division is to avoid the dependency of the Hamiltonian derivatives with respect to the coordinate q. By defining $p = (L - L_{eq})$, the reduced 1:1 resonance Hamiltonian can be written as

$$\mathcal{H} = \frac{1}{2}\mathcal{H}_0^{''}p^2 - b(\lambda)\cos q + fq \tag{30}$$

3.2.1 Fundamental resonance model

The last expression in Eq. 30 is the one related to a forced pendulum. We want to make the quadratic term of the Hamiltonian parameter free, so we perform a canonical transformation

$$(q, p, \mathcal{H}, t) \rightarrow (Q, P, \mathcal{K}, \tau) \tag{31}$$

with the condition

$$pdq - \mathcal{H}dt = \alpha(PdQ - \mathcal{K}d\tau) \tag{32}$$

and the new parameters are defined as

$$\begin{cases} P = c_2 p \\ \tau = c_1 t \\ q = Q + k\pi \end{cases} \tag{33}$$

So

$$pdq - \mathcal{H}dt = \frac{P}{c_2}dQ - \frac{\mathcal{H}}{c_1}\tau \tag{34}$$

$$= \frac{1}{c_2}(PdQ - \frac{c_2}{c_1}\mathcal{H}\tau) \tag{35}$$

Therefore, $\alpha = 1/c_2$ and the new Hamiltonian $\mathcal{K}$ can be derived as

$$\mathcal{K} = \frac{c_2}{c_1}\mathcal{H}_0^{''}\mathcal{H} \tag{36}$$

$$= \frac{\mathcal{H}_0^{''}}{c_1 c_2}\frac{1}{2}P^2 - \frac{c_2}{c_1}b\cos k\pi\cos Q \pm \frac{c_2}{c_1}fQ \tag{37}$$

Then, we fix

$$\frac{\mathcal{H}_0^{''}}{c_1 c_2} = 1 \quad \rightarrow \quad c_2 = \frac{\mathcal{H}_0^{''}}{c_1} \tag{38}$$

We define $t = \tau$, so $c_1 = 1$ and the Hamiltonian expression changes as

$$\mathcal{K} = \frac{1}{2}P^2 - \mathcal{H}_0^{''}b\cos k\pi\cos Q \pm \mathcal{H}_0^{''}fQ \tag{39}$$

$$= \frac{1}{2}P^2 - \omega^2\cos Q \pm f^* Q \tag{40}$$

where

$$\omega^2 = \mathcal{H}_0^{''}b\cos k\pi \quad , \quad f^* = \pm\mathcal{H}_0^{''}f \tag{41}$$

We choose $k = 0, 1$ to mantain the value of the frequency ω positive. If $k = 0$, we will choose the positive sign and if $k = 1$ the sign will be negative.
The equation of motion relative to the Hamiltonian in Eq.40 is

$$\ddot{Q} + \omega^2\sin Q = -f^* \tag{42}$$

3.3 Area variation with respect to λ

For the estimation of the probability of capture we refer to [7]. The equation of motion relative to the pendulum problem considered is

$$\ddot{\theta} + \omega^2\sin\theta = -\delta\beta \tag{43}$$

where $\beta > 0$, $d\lambda/dt = \delta$ and $0 < \delta \ll 1$. Comparing Eq.42 and Eq.43, we define

$$\beta = \frac{f^*}{\delta} \tag{44}$$

From the previous section we notice that $\delta = \epsilon$.
We define A_{res} as the libration region's area, A_{circ}^{up} as the upper circulation region's area and A_{circ}^{low} as the lower cir-

culation region's area. These are defined as [17]

$$\frac{d}{d\lambda}A^{up}_{circ} = \frac{d}{d\lambda}\left(-\int_{-\pi}^{\pi} P_+ dQ\right) \quad (45)$$

$$= \frac{d}{d\lambda}(-2\pi\beta - 8\omega) \quad (46)$$

$$\frac{d}{d\lambda}A_{res} = \frac{d}{d\lambda}\left(\int_{-\pi}^{\pi} (P_+ - P_-) dQ\right) \quad (47)$$

$$= \frac{d}{d\lambda}(16\omega) \quad (48)$$

$$\frac{d}{d\lambda}A^{low}_{circ} = \frac{d}{d\lambda}\left(\int_{-\pi}^{\pi} P_- dQ\right) \quad (49)$$

$$= \frac{d}{d\lambda}(2\pi\beta - 8\omega) \quad (50)$$

in which we dropped the constant terms. The expression of P_+ and P_- can be obtained from $\mathcal{K}$ in Eq.40 as

$$P_\pm(Q,\lambda) = \alpha \pm 2\omega \cos\frac{Q}{2} \quad (51)$$

where $\alpha = \int_0^t < \tau > dt$ [6].

3.4 Probability of capture

Fixing a region of the phase space, which includes the libration region, the probability of capture into resonance is directly related to the growth of the separatrices' size. From Liouville's Theorem, we deduce the expression of the probability of capture from the number of trajectories that cross the separatrix and are captured inside the libration region A_{res} as

$$Pr = -\frac{dA_{res}/d\lambda}{dA_0/d\lambda} \quad (52)$$

where A_0 is the area from which the trajectory crosses the separatrix. So the explicit expression for the probability of capture for the first fundamental resonance model, for $d\omega/d\lambda > 0$, is

$$Pr = \frac{8\frac{d\omega}{d\lambda}}{4\frac{d\omega}{d\lambda} + \pi\beta} \quad (53)$$

for $d\omega/d\lambda < \pi\beta/4$; while if $d\omega/d\lambda \geq \pi\beta/4$ the probability of capture $Pr = 1$. Finally, for $d\omega/d\lambda \leq 0$ the probability of capture $Pr = 0$.

4 Application

In this section we apply the AIT to estimate Dawn's probability of capture into resonance during its descent from HAMO to LAMO. As previously discussed in Section 2, We estimated numerically the probability to be 8.6% considering the initial conditions in Table 1. Considering Eq.25 and defining $q = 2\sigma$, for a polar and circular orbit the Hamiltonian reduces to

$$\mathcal{H}_{1:1} = -\frac{\mu^2}{2L^2} - \frac{3}{4}R_e^2\frac{\mu^4}{L_0^6(1-\lambda)^3}C_{22}\cos q - \dot{\theta}L + \frac{1}{2}\frac{T}{m}\frac{L^2}{\mu}q \quad (54)$$

The complete Hamiltonian is divided in three terms as follows

$$\mathcal{H}_0 = -\frac{\mu^2}{2L^2} - \dot{\vartheta}L \quad (55)$$

$$\mathcal{H}_{22} = -\frac{3}{4}R_e^2\frac{\mu^4}{L_0^6(1-\lambda)^3}C_{22}\cos q \quad (56)$$

$$\mathcal{H}_{LT} = \frac{1}{2}\frac{T}{m}\frac{L^2}{\mu}q \quad (57)$$

and we expand the $\mathcal{H}_0$ up to the second order, keeping only the quadratic term, and we expand $\mathcal{H}_{LT}$ to the order zero, thus considering only the constant term

$$\mathcal{H}_0^* = -\frac{3}{2}\frac{\mu^2}{L_{eq}^4} \quad , \quad \mathcal{H}_{LT}^* = \frac{1}{2}\frac{T}{m}\frac{L_{eq}^2}{\mu}q \quad (58)$$

So

$$\mathcal{H}_0^{''}|_{L_{eq}} = -3\frac{\mu^2}{L_{eq}^4} \quad (59)$$

$$b(\lambda) = \frac{3}{4}R_e^2\frac{\mu^4}{L_0^6(1-\lambda)^3}C_{22}\cos q \quad (60)$$

$$f = \frac{1}{2}\frac{T}{m}\frac{L_{eq}^2}{\mu} \quad (61)$$

We define the frequency and forcing term of the first fundamental resonance model considering $k = 1$, so that $\omega > 0$

$$\omega^2 = -\mathcal{H}_0^{''}|_{L_{eq}}b(\lambda) = \frac{9C_{22}\mu^6R_e^2}{4L_0^6L_{eq}^4(1-\lambda)^3} \quad (62)$$

$$f^* = -\mathcal{H}_0^{''}|_{L_{eq}}f = \frac{3}{2}\frac{T}{m}\frac{\mu}{L_{eq}^2} \quad (63)$$

Finally

$$\beta = \frac{f^*}{\epsilon} = \frac{3}{2}\frac{T}{m}\frac{\mu}{L_{eq}^2}\frac{a_0}{|\dot{a}|} \quad (64)$$

The derivative of the frequency with respect to λ in Eq.53 has to be evaluated at the time epoch in which the system crosses the separatrix. So, we numerically estimate the moment in which Dawn enters into resonance with Vesta. With the initial conditions defined in Table 1, the interval of time in which Dawn crosses the separatrix is 25.3 days and 27.4 days. Considering the minimum, mean and maximum values of the interval and using Eq.53 we estimate the probability of capture into resonance in Table 2.

Table 2: Estimation of the probability of capture into resonance of Dawn around Vesta.

Resonance crossing	Probability	Relative error
$t^*_{min} = 25.3$ days	7.5%	12.3%
$t^*_{mean} = 26.2$ days	7.68%	10.7%
$t^*_{max} = 27.4$ days	7.93%	7.8%

The table shows that considering only the tesseral harmonic from the spherical harmonic expansion the relative error between numerical (8.6%) and analytical estimates is about $8\% - 12\%$. We refine the Hamiltonian model including also the Hamiltonian term relative to the zonal harmonic contribution J_2 in the circular polar case

$$\mathcal{H}_{20} = -\frac{1}{4} R_e^2 \frac{\mu^4}{L^6} C_{20} \tag{65}$$

In a similar way, we obtain the resonance capture probability values in Table 3.

Table 3: Estimation of the probability of capture into resonance of Dawn around Vesta including zonal harmonic J_2.

Resonance crossing	Probability	Relative error
$t^*_{min} = 25.3$ days	7.78%	9.5%
$t^*_{mean} = 26.2$ days	7.98%	7.2%
$t^*_{max} = 27.4$ days	8.24%	4.1%

With the complete model the analytical estimates are closer to the numerical results. Specifically, the relative error decreases to about $4\% - 9\%$ between the two methodologies. Numerous approximations have been made in the estimation process that can justify the error that affects the analytical results: the Hamiltonian term relative to the low-thrust can be improved, the approximation of the SMA evolution is characterized by a 6% error and the Hamiltonian expansions around the resonance introduced errors due to truncations.

5 Conclusion

In this paper we present a new approach for estimating the probability of capture into resonance. The methodology is based on the adiabatic invariant theory, with which it is possible to estimate the probability of capture into resonance by analyzing the energy change of the dynamical system as it crosses the resonance. The one degree of freedom Hamiltonian model is composed by the natural part and a forced part related to the low-thrust. The estimation process requires to identify a parameter that slowly changes with time and the semi-major axis was considered as a good candidate for that role. We assumed a linear change in the semi-major axis evolution and compared it with the numerical simulation. We computed the area change of the resonance region and estimated the probability of capture into 1:1 resonance. The results show that by using this one degree of freedom Hamiltonian model we were able to estimate the probability of capture into 1:1 resonance for the nominal case of circular and polar orbit. The relative error between the numerical and analytical estimation is about 4%. In the paper, this methodology shows its potential to be used in astrodynamics.

Acknowledgements

We thank A. Neishtadt and S. Breiter for their expertise and helpful discussions for certain aspects of our study. This work is funded by ESA OSIP with project title ”Resonance Capture of Low-Thrust Spacecraft Around a Small Body” and by the John Anderson Research Award Studentship.

References

[1] C. Russell, “Dawn mission to vesta and ceres,” *Earth Moon Planet*, p. 65–91, 2007.

[2] N. Delsate, “Analytical and numerical study of the ground-track resonances of dawn orbiting vesta,” *Planetary and Space Science*, vol. 59, pp. 1372–1383, 2011.

[3] B. Garfinkel, “Regularization in the ideal resonance problem,” *Celestial Mechanics*, pp. 189–203, 1971.

[4] C. Yoder, “Diagrammatic theory of transition of pendulum like systems,” *Celestial Mechanics*, pp. 3–20, 1979.

[5] J. Henrard, “The adiabatic invariant: its use in celestial mechanics,” *Applications of Modem Dynamics to Celestial Mechanics and Astrodynamics*, pp. 153–171, 1982.

[6] Henrard, “Capture into resonance: an extension of the use of adiabatic invariants,” *Celestial Mechanics*, pp. 3–22, 1982.

[7] A. Neishtadt, “Passage through a separatrix in a resonance problem with a slowly-varying parameter,” *Journal of Applied Mathematics and Mechanics*, p. 594–605, 1975.

[8] D. Dobrott and J. M. Greene, “Probability of trapping-state transitions in a toroidal device,” *The Physics of Fluids*, vol. 14, p. 1525–1531, 1971.

[9] S. Breiter, “Fundamental models of resonance,” *Monografia de la Real Academia de Ciencias de Zaragoza*, p. 83–92, 2003.

[10] A. Artemyev, “Trapping (capture) into resonance and scattering on resonance: summary of results for space plasma systems,” *Communications in Nonlinear Science and Numerical Simulation*, vol. 65, pp. 111–160, 2018.

[11] D. Boccaletti and G. Pucacco, *Theory of Orbits: Perturbative and Geometrical Methods*. Springer Nature, 2010.

[12] W. M. Kaula, *Theory of Satellite Geodesy: Applications of Satellites to Geodesy*, 1966.

[13] P. Tricarico and M. Sykes, “The dynamical environment of dawn at vesta,” *Planetary and Space Science*, vol. 58, pp. 1516–1525, 2010.

[14] F. Capoani, “Adiabatic theory for slowly varying hamiltonian systems with applications to beam dynamics,” Bologna, Italy, 2017.

[15] C. Quillen, “Reducing the probability of capture into resonance,” *Monthly Notices of the Royal Astronomical Society*, pp. 1367–1382, 2006.

[16] A. Lemaître, “Resonances: Models and captures,” *Dynamics of Small Solar System Bodies and Exoplanets. Lecture Notes in Physics*, vol. 790, 2010.

[17] T. Eichmann, E. P. Thesing, and J. R. Anglin, “Engineering separatrix volume as a control technique for dynamical transitions,” *Physical Review*, vol. 98, 2021.